Potassium-modified calcium-ferrate-catalyzed hydrogenation of carbon dioxide to produce light olefins

Aixin Cui[a], Man Wu[a], Tuo Guo[a,b*], Xiunan Sun[c], Yulong Chen[a], Qingjie Guo[a,b*]

[a] *Laboratory of Green & Smart Chemical Engineering in Universities of Shandong, College of Chemical Engineering, Qingdao University of Science and Technology, Qingdao, Shandong 266042, China*

[b] *Xinyuan Green Carbon Technology (Jiangmen) Co., Ltd, Jiangmen, 529199, China.*

[c] *College of Energy and Chemical Engineering, Ningxia Vocational Technical College of Industry and Commerce, Yinchuan 750021, China.*

*Corresponding author.

Address: 53 Zhengzhou Road, Shibei District, Qingdao, 266042, Shandong, China.

E-mail address: qingjie_guo@vip.sina.com (Qingjie Guo);

tuo.guo.20@alumni.ucl.ac.uk (Tuo Guo)

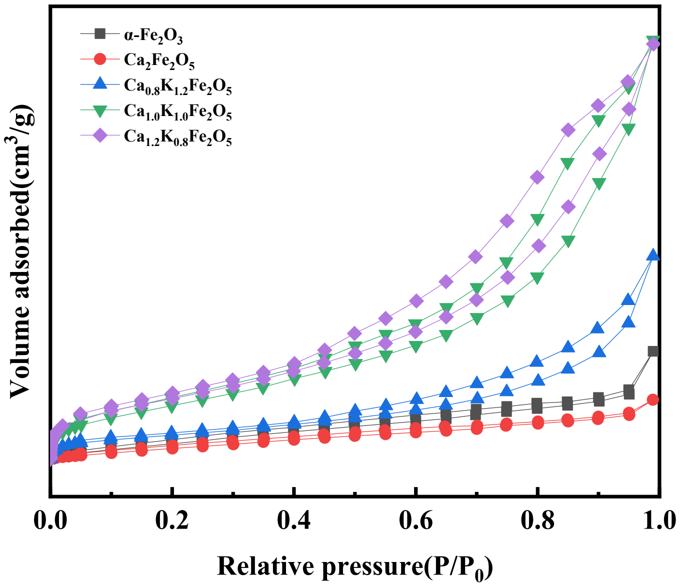

Fig. S1 N_2 adsorption-desorption isotherms of the samples

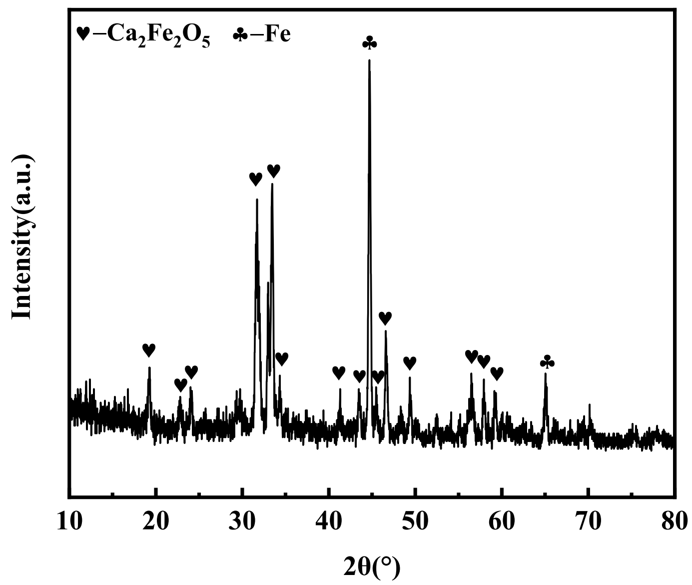

Fig. S2 XRD pattern of $Ca_{1.0}K_{1.0}Fe_2O_5$ catalyst reduction at 520°C

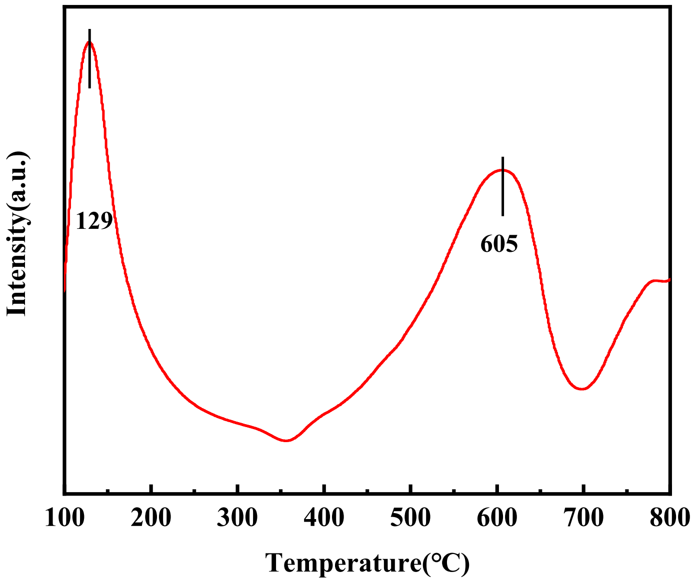

Fig. S3 CO_2-TPD of the K/α-Fe_2O_3 catalysts.

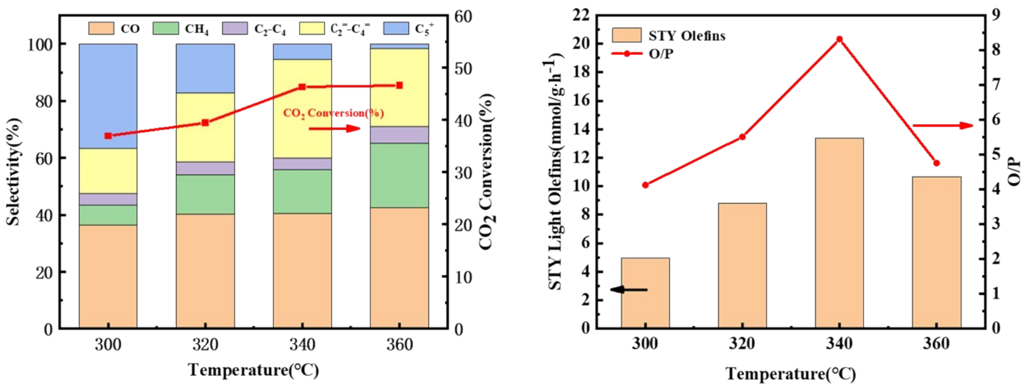

Fig. S4 Effect of temperature on conversion and selectivity over $Ca_{1.0}K_{1.0}Fe_2O_5$

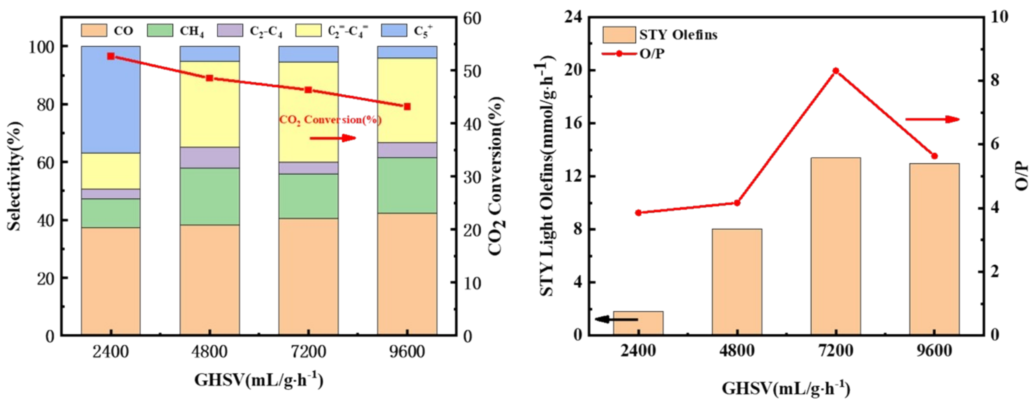

Fig. S5 Effect of GHSV conversion and selectivity over $Ca_{1.0}K_{1.0}Fe_2O_5$

The effects of temperature and airspeed on catalyst performance are depicted in **Fig S4** and **Fig S5**. The reaction temperature increased from 300°C to 360°C, the CO_2 conversion rate increased from 36.94% to 46.57%, and the CO selectivity increased from 36.34% to 42.56%. Meanwhile, the selectivity of light olefins increased first and then decreased. This is due to the fact that the first step reaction of CO_2 hydrogenation: RWGS is a heat-absorbing reaction, and an increase in temperature favors the RWGS reaction. Elevated temperature leads to more CO and H_2O being produced in the RWGS reaction, and CO accelerates the FT reaction, resulting in more hydrocarbons being produced. Although the higher temperature is more favorable for the generation of olefins, it also promotes the growth of carbon chains, which makes the proportion of light olefins in the products decrease. By comparing the selectivity of the reaction products at different temperatures, 340°C is more favorable for the generation of light olefins. In addition, the $Ca_{1.0}K_{1.0}Fe_2O_5$ catalyst had the highest $STY^{=}$ value (13.40 $mmol \cdot g^{-1} \cdot h^{-1}$) at 340°C, which means that 340°C is the optimal temperature for the catalytic preparation of light olefins from CO_2 with this catalyst.

The time of contact between the catalyst surface and the reactants had a significant effect on the conversion and selectivity of the products. Due to the decrease in the contact time between the reactants and the catalyst, the CO_2 conversion slightly decreased from 52.69% to 43.19% and the CO selectivity increased from 37.21% to 42.37% with the increase of GHSV. At the same time, the selectivity of light olefins firstly increased to 34.25% and then decreased to 29.20%, and the O/P value also decreased from 8.31 to 5.64. This was due to the high airspeed, the residence time of CO_2 and H_2 molecules on the catalyst was too short, and the molecules left the surface of the catalyst before completing the catalytic reaction. Moreover, the $STY^{=}$ of light olefin is highest at 7200 $mL \cdot g_{cat}^{-1} \cdot h^{-1}$, which is 13.4 $mmol \cdot g^{-1} \cdot h^{-1}$. Therefore, the optimum reaction space velocity for $Ca_{1.0}K_{1.0}Fe_2O_5$ catalyst is 7200 $mL \cdot g_{cat}^{-1} \cdot h^{-1}$.

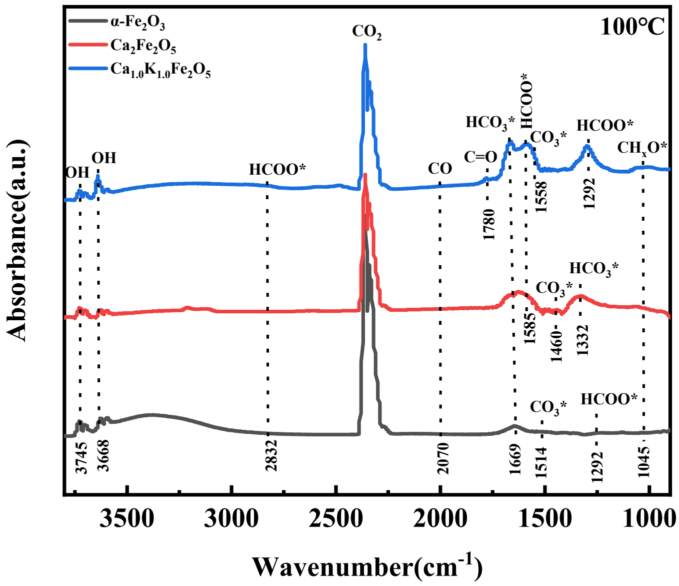

Fig. S6 *In situ* DRIFTS analysis of three reduced samples at 100°C

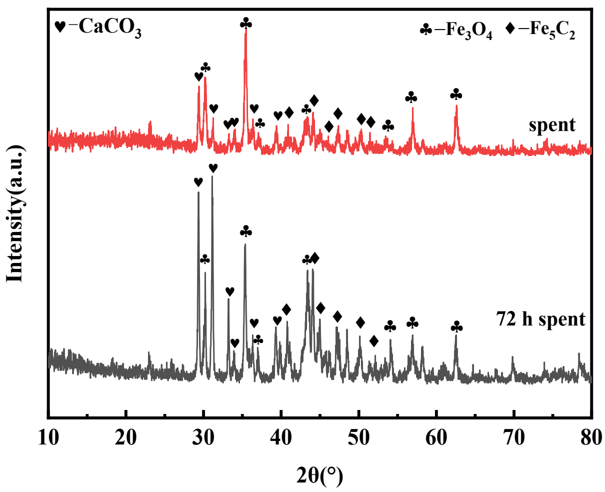

Fig. S7 XRD pattern of $Ca_{1.0}K_{1.0}Fe_2O_5$ catalyst after reaction and 72 h cycle

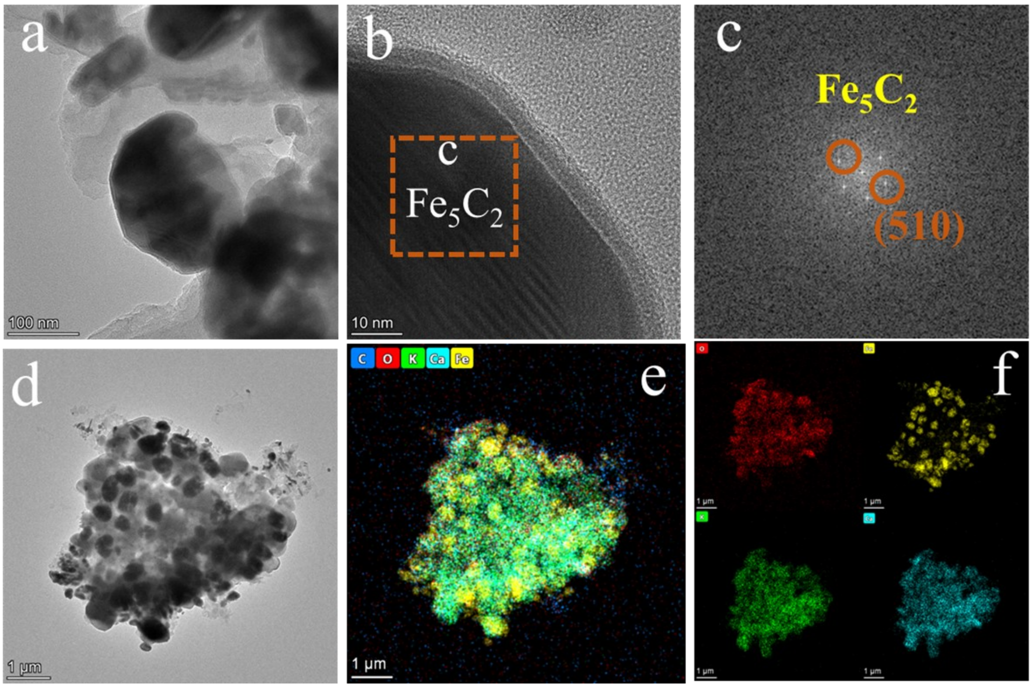

Fig. S8 HRTEM and EDS images of spent $Ca_{1.0}K_{1.0}Fe_2O_5$: (a-c) HRTEM. (d-f) EDS: (e) All, (f) O, Fe, K, Ca.

Table S1 Texture properties of catalysts mesoporous materials

Catalyst	**S_{BET}[a] ($m^2 \cdot g^{-1}$)**	**PV[b] ($cm^3 \cdot g^{-1}$)**	**PD[b] (nm)**
α-Fe_2O_3	22.9	0.04	7.7
$Ca_2Fe_2O_5$	17.5	0.02	5.5
$Ca_{0.8}K_{1.2}Fe_2O_5$	24.1	0.08	13.8
$Ca_{1.0}K_{1.0}Fe_2O_5$	56.4	0.17	12.2
$Ca_{1.2}K_{0.8}Fe_2O_5$	59.6	0.17	11.0

a: BET specific surface area;

b: total pore volume and average pore diameter calculated from the desorption branch of the isotherm using the BJH method;

Table S2 Percentage of $Fe_{2p3/2}$ of spent catalyst

Samples	$Fe_{2p3/2}$(%)		
	Fe^{2+}	Fe^{3+}	FeC_x
α-Fe_2O_3	79.16	15.09	5.75
$Ca_2Fe_2O_5$	55.33	34.60	10.08
$Ca_{1.2}K_{0.8}Fe_2O_5$	52.54	33.32	14.14
$Ca_{1.0}K_{1.0}Fe_2O_5$	67.49	17.67	14.84
$Ca_{0.8}K_{1.2}Fe_2O_5$	52.58	37.19	10.23

Table S3 Percentage of O1s of reduced catalyst

Samples	O1s(%)		
	O_{OH}	O_{ads}	O_{latt}
α-Fe_2O_3	16.23	29.05	54.72
$Ca_2Fe_2O_5$	12.54	51.01	36.45
$Ca_{1.2}K_{0.8}Fe_2O_5$	4.94	58.66	36.40
$Ca_{1.0}K_{1.0}Fe_2O_5$	8.48	61.66	16.87
$Ca_{0.8}K_{1.2}Fe_2O_5$	11.53	59.66	28.81

Table S4 Catalytic activity of the Fe-based catalysts.

Sample	**CO_2 Conv. (%)**	**Selectivity (%)**					**$STY^{=}$ ($mmol \cdot g^{-1} \cdot h^{-1}$)**	**O/P**
		CO	**CH_4**	**C_2^0 - C_4^0**	**$C_2^=$ - $C_4^=$**	**C_5^+**		
α-Fe_2O_3	34.55	27.92	36.85	31.49	3.33	0.41	0.96	0.11
K/Fe_2O_3	38.00	50.28	12.67	6.33	24.43	5.39	7.46	3.86
$Ca_2Fe_2O_5$	37.38	56.32	23.46	13.84	5.94	0.44	1.86	0.43
$Ca_{0.8}K_{1.2}Fe_2O_5$	40.48	43.67	22.96	4.91	25.35	3.12	8.58	5.16
$Ca_{1.0}K_{1.0}Fe_2O_5$	46.33	40.43	15.35	4.16	34.59	5.47	13.4	8.31
$Ca_{1.2}K_{0.8}Fe_2O_5$	43.30	42.67	18.18	5.39	26.49	7.27	9.59	4.91

Reaction parameters: H_2/CO_2 = 3; T = 340°C; P = 1.5 MPa; GHSV= 7200 $mL \cdot g_{cat}^{-1} \cdot h^{-1}$

Table S5 Comparison of catalytic performance of different catalysts

Catalysts	**T (°C)**	**P （MPa）**	**CO_2 Con.(%)**	**$C_2^=$ - $C_4^=$ Sel.(%)**	**O/P**	**Ref.**
$K/La_{0.4}Co_{0.4}Fe_{0.6}O_3$	320	2.0	36.00	29.31	1.95	1
Na-Mn-$CuFeO_2$	320	2.0	36.60	35.70	3.90	2
K-$CoFe_2O_4$	320	3.0	46.80	27.50	1.23	3
Na-$CoFe_2O_4$	320	3.0	41.80	37.20	5.39	4
K-$ZnCo_{0.5}Fe_{1.5}O_4$	320	2.5	49.60	36.1	5.82	5
$Sr_{0.6}K_{0.4}FeO_3$	350	1.0	30.82	29.61	5.48	6
$Ca_{1.0}K_{1.0}Fe_2O_5$	340	1.5	46.33	34.59	8.31	This work

Reference:

1. X. Sun, T. Guo, M. An, X. Guo, Z. Han, D. Zhai, J. Ma, X. Hu, J. Zhang, Y. He and Q. Guo, *Int. J. Hydrog. Energy*, 2024, **51**, 368-381.

2. G. Singh, D. Khurana, T. S. Khan, I. K. Ghosh, B. Chowdhury, A. Y. Khodakov and A. Bordoloi, *Applied Surface Science*, 2023, **616**.

3. M. Z. M. Wang, F. Ding, F. Yuan, G. Zhang, X. Nie, X. Guo,, *Low-Carbon*

Chemistry and Chemical Engineering, 2023, **48**, 41-49.
4. F. Yuan, G. Zhang, J. Zhu, F. Ding, A. Zhang, C. Song and X. Guo, *Catalysis Today*, 2021, **371**, 142-149.
5. Q. Q. Xu, X. Q. Xu, G. L. Fan, L. Yang and F. Li, *J. Catal.*, 2021, **400**, 355-366.
6. X. W. Y. Hou, M. Chen, X. Gao, Y. Liu, Q. Guo,, *Atmosphere*, 2022, **13**, 760.